Structure of White Dwarf Stars

Tom Wilson
School of Physics and Astronomy
University of Southampton

March 24, 2017

Abstract
We have used the Runge-Kutta method to model the mass and density profiles of white dwarf stars. These have been compared with case studies Sirius B, 40 Eri B and Stein 2051. It has been found that they are compatible. Our model supports the existence of a maximum possible mass for white dwarfs, the Chandrasekhar limit.

1. Introduction
The Structure of white dwarf stars is dependent on two main forces: the gravity of the star and the electron degeneracy pressure. When these two opposing forces are in equilibrium, the star is stable. From this model we can derive two differential equations describing the mass and density profiles:

$$\frac{d\rho}{dr} = -\left(\frac{dP}{d\rho}\right)^{-1} \frac{Gm}{r^2}\rho \qquad\qquad \frac{dm}{dr} = 4\pi r^2 \rho$$

where

$$\frac{dP}{d\rho} = Y_e \frac{m_e c^2}{m_p} \gamma\left(\frac{\rho}{\rho_0}\right) \qquad\qquad \gamma(y) = \frac{y^{2/3}}{3(1+y^{2/3})^{1/2}}$$

The third equation is an equation of state where Y_e is the average number of electrons per nucleon, thus being determined by the chemical composition of the star. The two differential equations can be solved numerically to give the mass and density profiles, including the total radius and mass of the star. This is in order to investigate how varying chemical composition and

central density will affect the structure of the star, and to compare this theoretical model with observed data.
The Runge-Kutta method has been chosen to solve the pair of equations. It has a suitable level of accuracy necessary for this project, whilst still being reasonably fast. Simpler methods (such as the Euler method) may be generally quicker, but in order to achieve a reasonably accurate answer the step size would have to be decreased such that calculation time is much larger.

An overview of the physics of white dwarfs is given in the next section, including a brief explanation of the derivative equations. Section 3 describes the method of generating the profiles, with results given in section 4 and discussed in section 5.

2. Background

White dwarf stars are formed when main sequence stars lack enough hydrogen to continue fusion. Given that it is no longer supported by thermal pressure, the remnant stellar core undergoes gravitational collapse. The result is a very dense object with a radius much smaller than that of the sun. At this density the star is supported by electron degeneracy pressure, a consequence of the Pauli exclusion principle.

For the electron degeneracy pressure *P*, Newton's law of gravitation gives

$$\frac{dP}{dr} = -\frac{Gm(r)}{r^2}\rho(r)$$

It follows that

$$\frac{d\rho}{dr} = -\left(\frac{dP}{d\rho}\right)^{-1}\frac{Gm}{r^2}\rho$$

Given the high temperatures within the star, the electrons are free and highly energetic so we can approximate the matter to be relativistic free fermi gas, resulting in the equation of state as derived by S. Chandrasekhar.
The second derivative equation is reached by considering a thin spherical shell within the star.

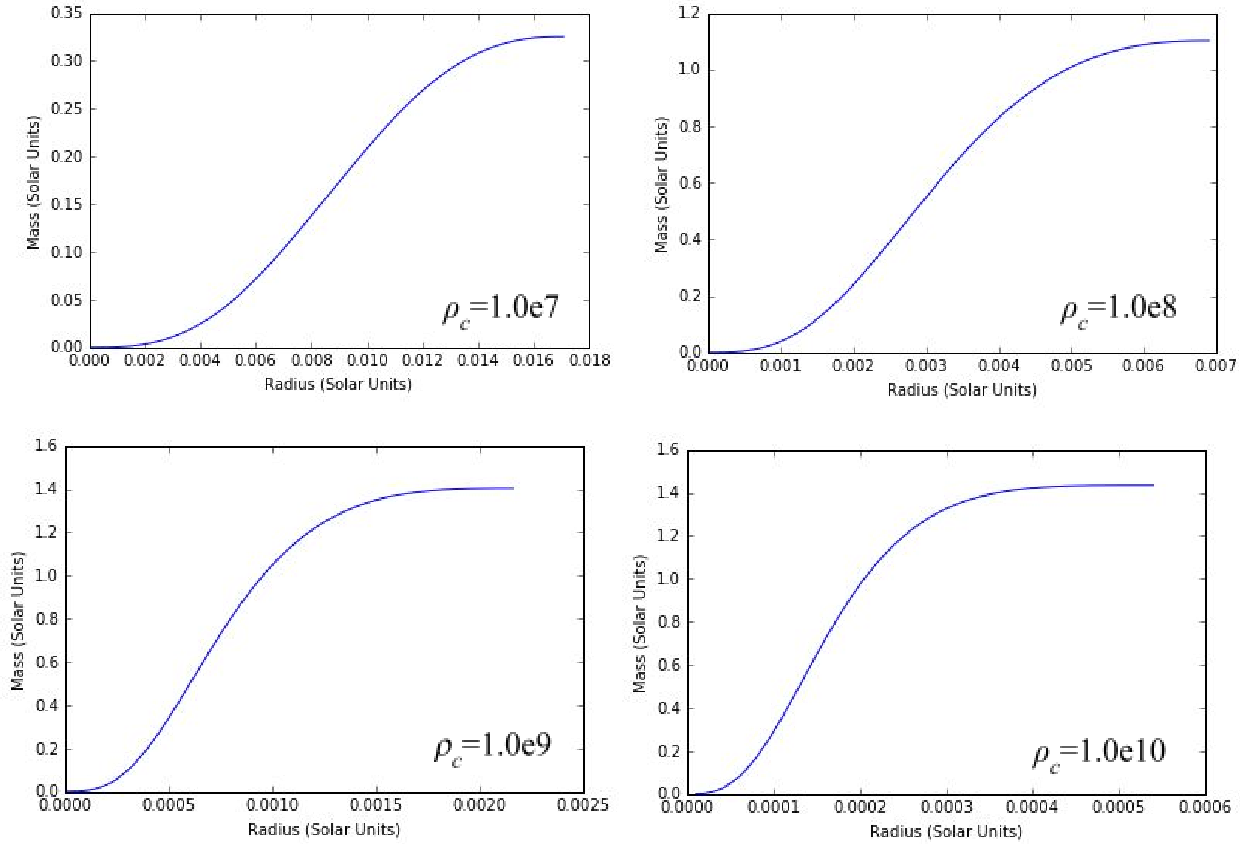

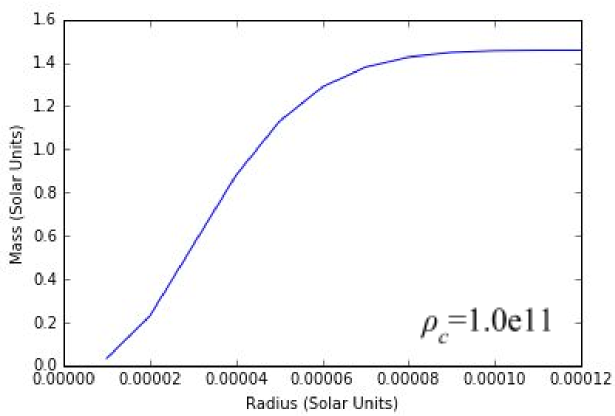

Figure 1 Mass profiles for varying ρ_c values.

3. Method

Initially we define $\varrho_0^{(-1/3)}$ and the gamma factor □, using solar units and ρ_c as a unit for density. A scaling factor is then defined for each differential equation

$$C_m = \frac{4\pi R_\odot^3 \rho_c}{M_\odot} \qquad\qquad C_\rho = -\frac{G m_p M_\odot}{Y_e m_e c^2 R_\odot}$$

combining constants and units into a single factor. This is done to ensure the variables are a reasonable size when the runge-kutta algorithm is applied, to avoid numerical errors. The derivative equations are thus defined:

$$\frac{d\rho}{dr} = \frac{C_\rho m \rho}{r^2 \gamma\left(\frac{\rho}{\rho_0}\right)} \qquad\qquad \frac{dm}{dr} = C_m r^2 \rho$$

The definition for the first derivative includes a condition setting it equal to zero if r=0, in order to avoid a zero division error at the beginning of the operation. Terms including ϱ use the absolute value to avoid an error in the final loop when ϱ is negative. The initial conditions are set as the center of the star, with some central density ρ_c and zero radius and mass. The runge-kutta method is applied to the equations, integrating them outwards until the program is terminated when the density value reaches zero, at the surface of the star.

The step size was reduced (by increasing N) until the results were not changing by a significant amount. Beyond the chosen step size ($h=0.00001$) the time taken for the program to execute increased considerably, without any appreciable increase in accuracy.

The central density is manually varied to find values that produce parameters matching the observed stars. The given errors have been propagated from those of the observable data. This repeated for Y_e=0.5 and Y_e=0.464. They represent a star dominated by carbon and iron, respectively.

4. Results

The figures show the mass profiles for stars of varying central density. As ρ_c is increased, the stars become much smaller. Their total mass increases with density only until a value of 1.43 $M_\odot$. As ρ_c is increased beyond this point the mass profile achieves this limit at a smaller radius, outside of which the density is very low. For higher ρ_c values, the mass profiles initial increase is much steeper.

We found that for Y_e=0.5, the observed Sirius B parameters were consistent with our model for a central density of ρ_c=8.50 ± 0.80 x 10^7 kg m^{-3}. The parameters for 40 Eri B and Stein 2051 were not consistent with our model. However, for Y_e=0.464 they were found to be consistent with ρ_c=2.15 ± 0.15 x 10^7 kg m^{-3} and ρ_c=2.33 ± 0.37 x 10^7 kg m^{-3}, respectively. Sirius B was found to be inconsistent with our model at Y_e=0.464. These results are displayed in table 1 and figure 2.

Figure 3 compares the mass and density profiles of a white dwarf of ρ_c=8.0 x 10^7 kg m^{-3} with different Y_e values. Increasing the number of electrons per nucleon will increase the density of the star at any radial distance, resulting in the mass profile rising sharply at outer radii. This has the effect of significantly increasing the total mass of the star, and slightly increasing its size.

	Central Density (x 10^7 kg m^{-3})
Sirius B	8.50 ± 0.80
40 Eri B	2.15 ± 0.15
Stein 2051	2.33 ± 0.37

Table 1 Calculated central density values

5. Discussion

It is found that as the central density is increased, the total mass of the star increases only until a limit of 1.43 $M_\odot$. This is known as the Chandrasekhar limit; the maximum mass possible for a stable white dwarf is about 1.44 $M_\odot$. Beyond this, the gravitational pressure is too great to be counterbalanced by the electron degeneracy pressure. Collapsing stars more massive than this limit will evolve into neutron stars or black holes. Thus our model supports the theoretical mass limit for stars evolving into white dwarfs.

Our model is consistent with observational findings, supporting the theory that white dwarfs are largely supported by electron degeneracy pressure. We find that the studied cases have a mass comparable to that of the sun but with a much smaller radius, and a denser center than the sun's (ρ_c=1.622 x 10^5 kg m^{-3}). This suggests that it contains heavier elements than those found in the sun, most likely Iron and Carbon.

6. Conclusion

We have utilised the runge-kutta method to give numerical solutions modelling the structure of a white dwarf star. Our model was found to be in agreement with observed data, supporting the theory that white dwarf structure is determined by electron degeneracy pressure. We investigated how chemical composition affects mass and size, concluding that those dominated by carbon will be larger and more massive than those dominated by iron. Our model also gives evidence supporting the validity of the Chandrasekhar limit.

References

S. Chandrasekhar, The highly collapsed configurations of a stellar mass (Second paper), *Monthly Notices of the Royal Astronomical Society*, **95**: 207–225 (1935)

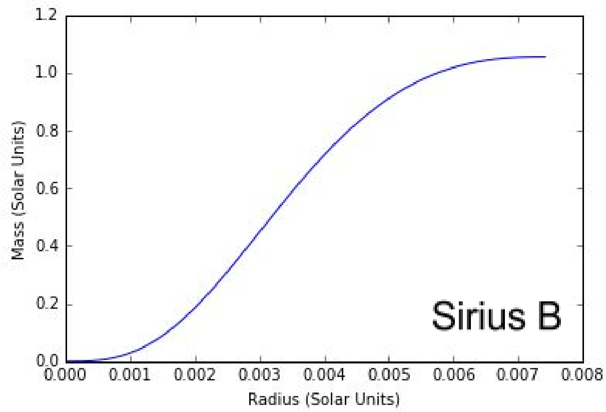

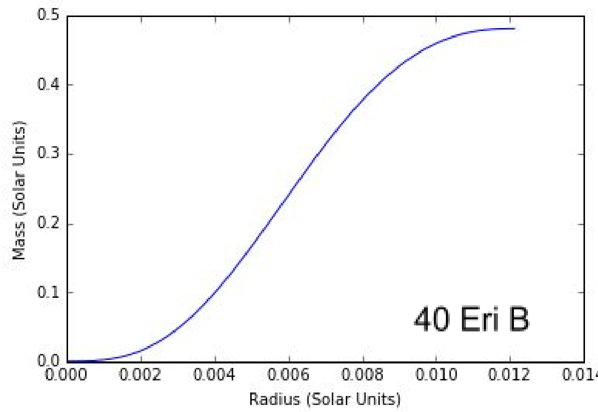

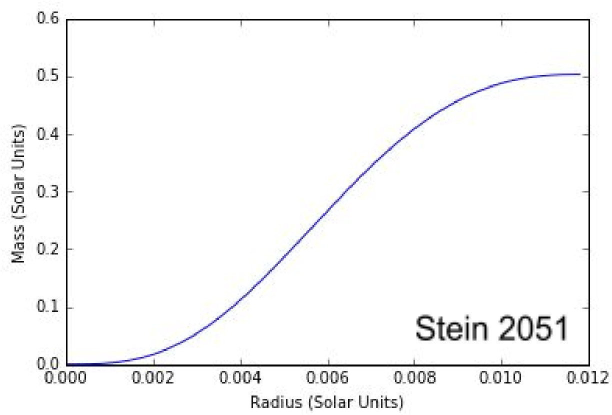

Figure 2 Modelled mass profiles for three white dwarfs

Figure 3 Mass and density profiles for Y_e=0.5 and Y_e=0.464